

Photon-axion oscillations and type Ia supernovae

Edvard Mörtzell,* Lars Bergström,† and Ariel Goobar‡

Department of Physics, Stockholm University, S-106 91 Stockholm, Sweden

(Received 27 February 2002; published 29 August 2002)

We compute the probability of photon-axion oscillations in the presence of both intergalactic magnetic fields and an electron plasma and investigate the effect on type Ia supernovae observations. The conversion probability is calculated using a density matrix formalism by following light paths through simulated universes in a Monte Carlo fashion. We find that, even though the effect is highly frequency dependent, one needs to analyze relatively narrow spectral features of high redshift objects in order to discriminate between the dimming effect from oscillations and a cosmological constant, in contrast with earlier claims that broadband photometry is sufficient. However, it should be possible to put severe constraints on the effect by studying, e.g., quasar-, gamma-ray burst-, and galaxy-spectra.

DOI: 10.1103/PhysRevD.66.047702

PACS number(s): 13.40.Hq, 97.60.Bw, 98.80.Es

I. INTRODUCTION

Recently, Csáki, Kaloper, and Terning [1] (CKT) proposed that the observed faintness of high redshift supernovae (SNe) could be attributed to the mixing of photons with a light axion in an intergalactic magnetic field. Assuming magnetic domains with an uncorrelated field direction of a size \sim Mpc, CKT found that for optical photons the oscillation is maximal and independent of energy, i.e., in the limit of infinite travel distance one approaches an equilibrium between the two photon polarization states and the axion. For optical photons, the probability to detect a photon as a function of the traveled distance l was approximated as

$$P_\gamma \approx \frac{2}{3} + \frac{1}{3} \exp(-l/l_0), \quad (1)$$

where l_0 is the exponential decay length. It was claimed that since this effect will cause additional dimming of high redshift SNe, constraints on the equation of state parameter of the dark energy component could be significantly relaxed. The presence of a nonclustering component of dark energy has recently been independently inferred from a combination of measurements of the cosmic microwave background and the distribution of galaxies on large scales. The proposed mechanism does not remove the need for such a component, but its equation of state need not be as close to that for a cosmological constant as is the case without such a mixing. For a magnetic field strength of $|\vec{B}| \sim 10^{-9}$ G, CKT found that the current data can be accommodated by $\Omega_M = 0.3, \Omega_X = 0.7, \omega_X = -1/3$ if the axion mass is $m \sim 10^{-16}$ eV and the coupling scale is $M \sim 4 \times 10^{11}$ GeV.

It was pointed out by Deffayet, Harari, Uzan, and Zaldarriaga [2] that one has to take the effect of the intergalactic plasma into account, i.e., the free electrons in which the photons are propagating. For a mean electron density of $n_e \sim 10^{-7}$ cm $^{-3}$, they found that this will lower the oscillation

probability and may also cause the oscillations for optical photons to be frequency dependent to a degree where the effect can be ruled out by studying the color excess between the B and V wavelength bands. Only for very definitive properties of the intergalactic magnetic field could one get a large enough mixing angle and weak enough frequency dependence, namely, with $|\vec{B}| \sim 10^{-8}$ G over domains of size ~ 10 kpc and weaker magnetic field strength over larger domains. (The strength and spatial properties of intergalactic magnetic fields are not well constrained by present measurements; for a recent review see [3].)

Csáki *et al.* [1,4] argue that the mean electron density in most of space realistically is lower than the estimate used by Deffayet *et al.* by a factor of at least 15, which is enough to bring the energy dependence within current experimental bounds.

In this paper, we perform a full density matrix calculation of the photon-axion oscillations and find the conversion probability to be highly frequency dependent and also not necessarily monotonically increasing with redshift. We also calculate the color excess between different wavelength bands for type Ia SNe by integrating over spectrum templates modified by performing the density matrix calculation over the appropriate frequency range (taking the redshifting of the spectra into account).

II. DENSITY MATRIX FORMALISM

We compute the mixing probability using the formalism of density matrices (see, e.g., [5]). Following the notation of [2], we define the mixing matrix as

$$M = \begin{pmatrix} \Delta_\perp & 0 & \Delta_M \cos \alpha \\ 0 & \Delta_\parallel & \Delta_M \sin \alpha \\ \Delta_M \cos \alpha & \Delta_M \sin \alpha & \Delta_m \end{pmatrix}. \quad (2)$$

The different quantities appearing in this matrix are given by

$$\Delta_\perp = -3.6 \times 10^{-25} \left(\frac{\omega}{1 \text{ eV}} \right)^{-1} \left(\frac{n_e}{10^{-8} \text{ cm}^{-3}} \right) \text{ cm}^{-1}, \quad (3)$$

*Electronic address: edvard@physto.se

†Electronic address: lbe@physto.se

‡Electronic address: ariel@physto.se

$$\Delta_{\parallel} = \Delta_{\perp}, \quad (4)$$

$$\Delta_{\text{M}} = 2 \times 10^{-26} \left(\frac{B_{0\perp}}{10^{-9} \text{ G}} \right) \left(\frac{M_{\text{a}}}{10^{11} \text{ GeV}} \right)^{-1} \text{ cm}^{-1}, \quad (5)$$

$$\Delta_{\text{m}} = -2.5 \times 10^{-28} \left(\frac{m_{\text{a}}}{10^{-16} \text{ eV}} \right)^2 \left(\frac{\omega}{1 \text{ eV}} \right)^{-1} \text{ cm}^{-1}, \quad (6)$$

where $B_{0\perp}$ is the strength of the magnetic field perpendicular to the direction of the photon, M_{a} is the inverse coupling between the photon and the axion, n_{e} is the electron density, m_{a} is the axion mass, and ω is the energy of the photon. The angle α is the angle between the (projected) magnetic field and the (arbitrary, but fixed) perpendicular polarization vector. Our standard set of parameter values is given by

$$\begin{aligned} B_0 &= 10^{-9} (1+z)^2 \text{ G}, \\ M_{\text{a}} &= 10^{11} \text{ GeV}, \\ m_{\text{a}} &= 10^{-16} \text{ eV}, \\ n_{\text{e}}(z) &= 10^{-8} (1+z)^3 \text{ cm}^{-3}, \end{aligned} \quad (7)$$

with a 20% dispersion in B_0 and n_{e} , and the redshift dependence of the magnetic field strength and the electron density comes from flux conservation and cosmological expansion, respectively. The equation to solve for the evolution of the density matrix ρ is given by

$$i\delta_t \rho = \frac{1}{2\omega} [M, \rho], \quad (8)$$

with initial conditions

$$\rho_0 = \begin{pmatrix} \frac{1}{2} & 0 & 0 \\ 0 & \frac{1}{2} & 0 \\ 0 & 0 & 0 \end{pmatrix}. \quad (9)$$

Here the three diagonal elements refer to two different polarization intensities and the axion intensity, respectively. We solve the system of nine coupled (complex) differential equations numerically [6], by following individual light paths through a large number of cells where the strength of the magnetic field and the electron density is determined from predefined distributions and the direction of the magnetic field is random. Through each cell the background cosmology and the wavelength of the photon are updated, as well as the matrices ρ and M . The cell sizes correspond to typical distances between galaxies, i.e., ~ 3 Mpc.

In order to study the qualitative behavior of the solutions, we rewrite M as a 2×2 matrix,

$$M^{2\text{D}} = \begin{pmatrix} \Delta & \Delta_{\text{M}} \\ \Delta_{\text{M}} & \Delta_{\text{m}} \end{pmatrix}, \quad (10)$$

where $\Delta = \Delta_{\perp} = \Delta_{\parallel}$ and Δ_{M} is the component of the magnetic field parallel to the average polarization vector of the photon beam. We solve Eq. (8) for the density matrix $\rho^{2\text{D}}$ with initial conditions

$$\rho_0 = \begin{pmatrix} 1 & 0 \\ 0 & 0 \end{pmatrix}, \quad (11)$$

where the diagonal elements refer to the photon and the axion intensity, respectively. Assuming a homogeneous magnetic field and electron density, we can solve the two-dimensional system analytically. For the $\rho_{11}^{2\text{D}}$ component, referring to the photon intensity, we get

$$\begin{aligned} \rho_{11}^{2\text{D}} &= 1 - \left(\frac{\Delta_{\text{M}}}{2\omega\Omega} \right)^2 (1 - \cos \Omega t), \\ \Omega &= \frac{\sqrt{(\Delta - \Delta_{\text{m}})^2 + 2\Delta_{\text{M}}^2}}{2\omega}. \end{aligned} \quad (12)$$

We see that we get maximal mixing if $\Delta = \Delta_{\text{m}}$, i.e., if $m_{\text{a}} = m_{\text{max}} \approx 38 \sqrt{n_{\text{e}} / (10^{-8} \text{ cm}^{-3})} 10^{-16} \text{ eV}$. For $m_{\text{a}} \gg m_{\text{max}}$, the oscillations are suppressed as m_{a}^{-4} . For $m_{\text{a}} \ll m_{\text{max}}$, the effect is insensitive to the values of the axion mass which our numerical simulations show is true even for $m_{\text{a}} \approx m_{\text{max}}$. For values close to the typical set of parameter values, we can set $\Omega \approx \Delta / (2\omega)$ to get

$$\rho_{11}^{2\text{D}} \approx 1 - \left(\frac{\Delta_{\text{M}}}{\Delta} \right)^2 \left(1 - \cos \frac{\Delta t}{2\omega} \right). \quad (13)$$

For small mixing angles, the effect should be roughly proportional to B_0^2 and M_{a}^{-2} , whereas the effect should be rather insensitive to the exact values of the input parameters in cases of close to maximal mixing. We also expect the effect to be stronger for low values of the electron density approaching maximal mixing for $n_{\text{e}} = 0$. These predictions are confirmed by numerical simulations. The oscillation length is of the order $\sim \text{Mpc}$, i.e., comparable to the size of the magnetic domains used in the numerical integration. In general, smaller magnetic domains (corresponding to smaller cell sizes) yield lower oscillation probabilities, in accordance with the results of Ref. [1].

III. RESULTS

In Fig. 1, we show the attenuation due to photon-axion oscillations as a function of wavelength for one specific line of sight for our standard set of input parameter values [see Eq. (7)] at $z = 0.1$ (upper panel), $z = 0.2$ (middle panel), and $z = 0.5$ (lower panel) in a $\Omega_{\text{M}} = 0.28$, $\Omega_{\Lambda} = 0.72$ universe, which is what we will use subsequently. We have performed a number of simulations using a wide range of cosmological parameter values and found the oscillation effect to depend only weakly on cosmology. The most dramatic effect is the

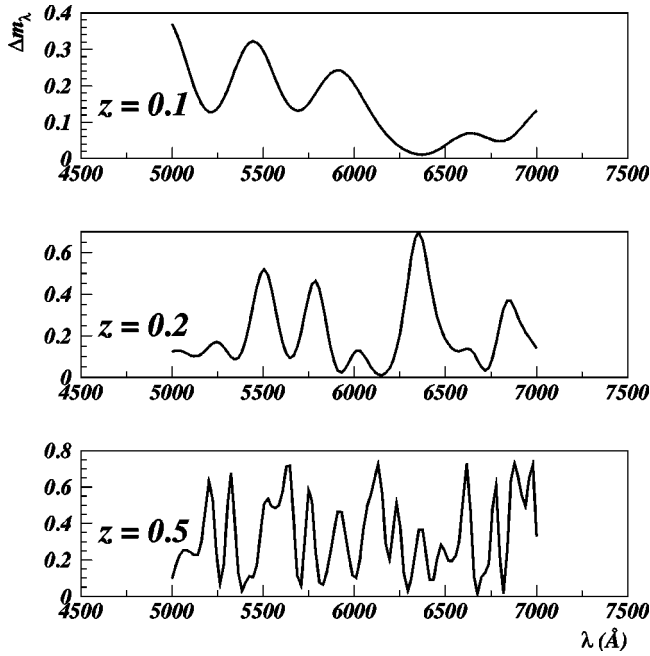


FIG. 1. The attenuation due to photon-axion oscillations for the standard set of parameter values [see Eq. (7)] as a function of wavelength at redshift $z=0.1$ (upper panel), $z=0.2$ (middle panel), and $z=0.5$ (lower panel).

strong variation of attenuation with photon energy.

Since the attenuation varies very rapidly with photon energy in a similar manner over a broad energy range, we expect the frequency dependence to wash out to a large extent when doing broadband photometry.

In Fig. 2, we show the source rest-frame B -band [i.e., the filter redshifted by a factor $(1+z)$ in wavelength] magnitude attenuation for type Ia SNe due to photon-axion oscillations for three different values of the electron density, in the redshift interval $0 < z < 2$, using values for the other input parameters from Eq. (7). Each point represents the average value and the error bars the dispersion for ten different lines of sight. In the upper panel, we have used $n_e = 10^{-7} \text{ cm}^{-3} (1+z)^3$, in the middle panel $n_e = 5 \times 10^{-8} \text{ cm}^{-3} (1+z)^3$, and in the lower panel $n_e = 10^{-8} \text{ cm}^{-3} (1+z)^3$. Note that the effect is not necessarily increasing with increasing redshift. This is due to the fact that we are studying the *rest-frame* B -band magnitude. Since the amplitude of the oscillations scales roughly as $(\omega/n_e)^2$ [see Eq. (13)], we need this combination to be large at some point in order to get close to maximal mixing. If the plasma density is high, the photon energy will be redshifted to too low energies before the plasma density is diluted due to the expansion.

In Fig. 3, the rest-frame B -band magnitude attenuation for type Ia SNe for three different values of the intergalactic field strength is shown. Again, each point represents the average value and the error bars the dispersion for ten different lines of sight. In the upper panel, $B_0 = 10^{-10} (1+z)^2 \text{ G}$, in the middle panel $B_0 = 5 \times 10^{-10} (1+z)^2 \text{ G}$, and in the lower panel $B_0 = 10^{-9} (1+z)^2 \text{ G}$. All other parameter values are given by Eq. (7).

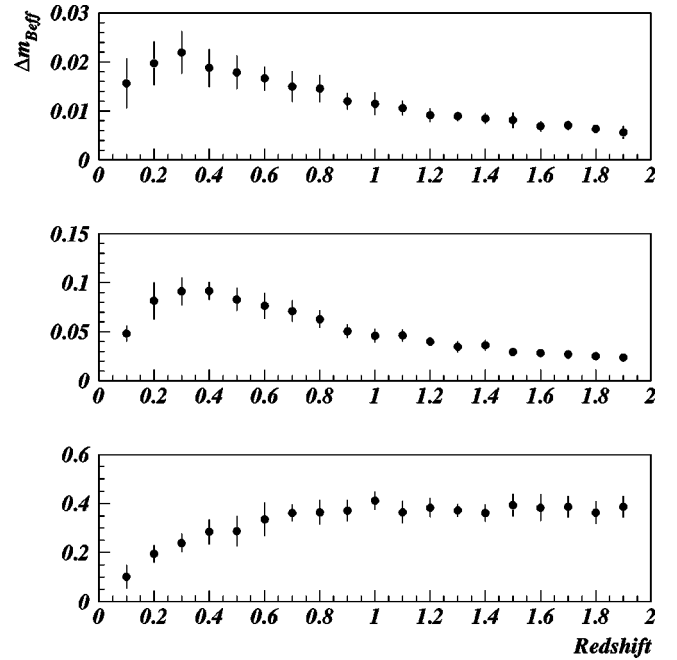


FIG. 2. The attenuation integrated over the rest-frame B -band of type Ia SNe due to photon-axion oscillations with $n_e = 10^{-7} (1+z)^3 \text{ cm}^{-3}$ (upper panel), $n_e = 5 \times 10^{-8} (1+z)^3 \text{ cm}^{-3}$ (middle panel), and $n_e = 10^{-8} (1+z)^3 \text{ cm}^{-3}$ (lower panel). All other parameter values are given by Eq. (7).

Our results indicate that we need low electron densities in order to get an attenuation that increases with redshift. One should keep in mind that the overall normalization can be set by varying the strength of the magnetic fields and/or the photon-axion coupling strength.

Based on a sample of 36 $z \sim 0.5$ SNe, Perlmutter *et al.* [7] measured the average rest-frame $B-V$ color excess to be $0.035 \pm 0.022 \text{ mag}$. We find the expected color excess with our standard set of parameters to be $E(B-V) = 0.006 \text{ mag}$, with a scatter around this value of 0.004 mag.

We can investigate the frequency dependence when doing broadband photometry by studying the extinction (at maximum intensity) in $V-J$, $R-J$, and $I-J$ for type Ia SNe as a function of redshift, as we show in Fig. 4. All the broadband filters and spectroscopy wavelength scales are in the observer's frame. We can see that in all three cases the color excess is very small and thus difficult to measure.

In general, the nature of the frequency dependence will depend on the exact values of the input parameters and the redshift with the possibility of generating both reddening and bluing. We thus conclude that it will be very difficult to use the color excess between different broadbands to put severe limits on the photon-axion mixing parameters.

IV. DISCUSSION

Our numerical simulations indicate that, in order to get a dimming effect from photon-axion oscillations similar to the one from a cosmological constant (increasing at lower redshifts, saturating at higher), one would need to have an average intergalactic electron density of $n_e \lesssim 10^{-8} \text{ cm}^{-3} (1$

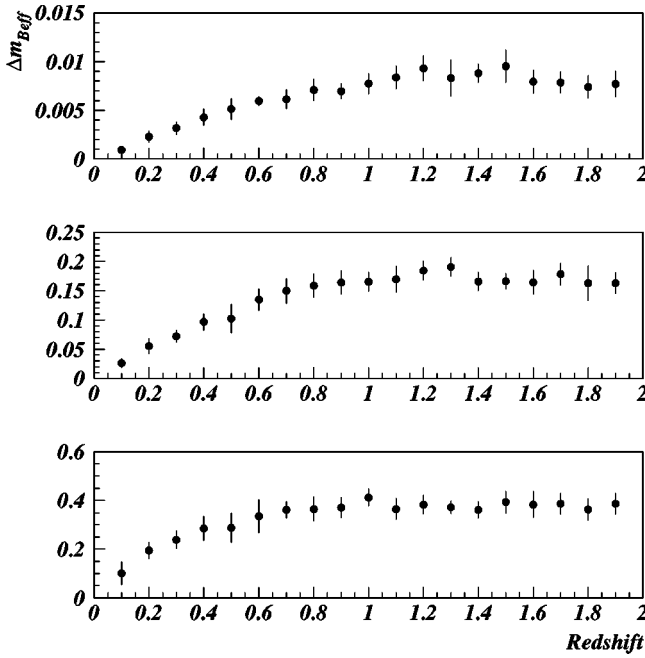


FIG. 3. The attenuation integrated over the rest-frame B band of type Ia SNe due to photon-axion oscillations with $B_0=10^{-10}(1+z)^2$ G (upper panel), $B_0=5 \times 10^{-10}(1+z)^2$ G (middle panel), and $B_0=10^{-9}(1+z)^2$ G (lower panel). All other parameter values are given by Eq. (7).

$+z)^3$. Assuming this, it should be possible to vary the average magnetic field strength or the photon-axion coupling strength in order to fit the current broadband photometry data. Note that in the case of close to maximal mixing, results are generally not very sensitive to the exact values of the input parameters, yielding results similar to the upper panel in Fig. 2.

Since photon-axion oscillations can cause either reddening or blueing (or no color excess at all) for close to maximal mixing and the integrated broadband magnitudes wash out the dispersion in attenuation, we expect spectroscopic studies of especially high- z objects to be a more powerful discriminator between different oscillation models and the case of a cosmological constant or any other dark energy component (for which we suppose the dimming to be entirely frequency independent). Systematic analysis of quasar-, gamma-ray burst-, and galaxy-spectra as a function of redshift by, e.g., the Sloan Digital Sky Survey and 2dF groups are probably

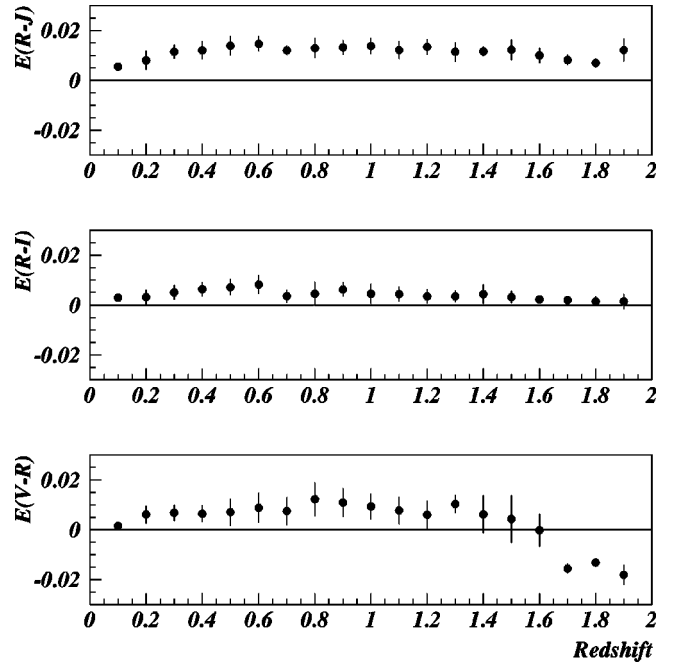


FIG. 4. Color extinctions $E(V-J)$, $E(R-J)$, and $E(I-J)$ for type Ia SNe as a function of redshift. Note that the dimming associated with photon-axion mixing, unlike extinction by dust, can also generate *blueing*.

the best probes for the photon-axion mixing parameter space. Note that the source size sets a lower limit to the size of the fluctuations that can be probed since the fluctuations will average out if photons from different parts of the source travel through different magnetic field strengths and electron densities.

Supernova spectra, available with good signal-to-noise ratios up to at least $z \sim 0.5$, are useful probes for the large mixing parameters that would yield a sufficient dimming of type Ia SNe as to explain the Hubble diagrams in [7,8] without invoking dark energy.

ACKNOWLEDGMENTS

We are grateful to S. Hansen for bringing the CKT paper to our attention, and to G. Raffelt for insightful comments improving the quality of the manuscript. We also wish to thank J. Edsjö, H. Rubinstein, C. Fransson, and J. Silk for helpful discussions. The research of L.B. is sponsored by the Swedish Research Council (VR). A.G. is supported by a grant from the Knut and Alice Wallenberg Foundation.

[1] C. Csáki, N. Kaloper, and J. Terning, Phys. Rev. Lett. **88**, 161302 (2002).
 [2] C. Deffayet, D. Harari, J. P. Uzan, and M. Zaldarriaga, this issue, Phys. Rev. D **66**, 043517 (2002).
 [3] D. Grasso and H. R. Rubinstein, Phys. Rep. **348**, 163 (2001).
 [4] C. Csáki, N. Kaloper, and J. Terning, Phys. Lett. B **535**, 33 (2002).

[5] J. J. Sakurai, *Modern Quantum Mechanics* (Addison-Wesley, Reading, MA, 1995).
 [6] We have used the LSODA package from Netlib, <http://www.netlib.org>
 [7] S. Perlmutter *et al.*, Astrophys. J. **517**, 565 (1999).
 [8] A. G. Riess *et al.*, Astron. J. **116**, 1009 (1998).